

1        INTERSPECIFIC VARIATION IN THE TIMING AND MAGNITUDE OF HYDRAULIC  
2                    REDISTRIBUTION IN A FOREST WITH DISTINCT WATER SOURCES

3 Michael Belovitch<sup>1,2,3</sup>, Steven Brantley<sup>3</sup>, and Doug. P. Aubrey<sup>1,2</sup>

4

5   <sup>1</sup>Warnell School of Forestry and Natural Resources, University of Georgia, Athens, Georgia,  
6 30602 USA

7   <sup>2</sup>Savannah River Ecology Laboratory, University of Georgia, Aiken, South Carolina, 29802 USA

8   <sup>3</sup>The Jones Center at Ichauway, Newton, Georgia, 39870 USA

9

10

11   \*Corresponding Author:

12 Michael Belovitch

13 Odum School of Ecology  
14 140 East Green Street  
15 Athens, GA 30602

16

17 Cell #: (571) 225-0682

18 Email: belovimw@gmail.com

19 **Abstract**

20 **Aims**

21 Trees regulate water availability among their rooting strata through a nocturnal, passive  
22 transference of water known as hydraulic redistribution (HR). This study investigates differences  
23 in HR and groundwater use among common canopy species in longleaf pine (*Pinus palustris* Mill.,  
24 Pinaceae) woodlands and explores environmental factors influencing HR.

25 **Methods**

26 HR was estimated by sap flux of lateral roots and main stems of three mature canopy  
27 species (*P. palustris*, *Quercus laevis* Walter., Fagaceae and *Quercus margarettae* Ashe.,  
28 Fagaceae). We used  $\delta^{18}\text{O}$  and  $\delta\text{D}$  of xylem water, soil water, and groundwater to determine water  
29 source. Finally, we related HR to environmental factors (Temperature, VWC, VPD) to better  
30 understand controls of HR dynamics.

31 **Results**

32 *Pinus palustris* had higher water use than either *Quercus* species, and also redistributed  
33 significantly more water as a nocturnal subsidy. HR fluxes were inversely related with mean daily  
34 temperature and independent of shallow soil moisture. Stable isotope mixing models, based on  
35  $\delta^{18}\text{O}$  and  $\delta\text{D}$ , indicated that all species have access to groundwater, but utilized shallow soil water  
36 in differing amounts when available.

37 **Conclusions**

38 In systems with strong water potential gradients among soil strata, any species with access  
39 to a groundwater source is likely capable of HR; however, the magnitude of HR varies significantly  
40 by species, even among closely related taxa.

41 Keywords: Hydraulic lift,  $\delta^{18}\text{O}$ ,  $\delta\text{D}$ , drought resistance, root profile, soil water content, hydrologic  
42 niche, groundwater use

## 43 **Introduction**

44           Hydraulic redistribution (HR) is a physical process wherein water is transferred across the  
45 soil profile through a plant's roots (Caldwell et al. 1998). HR occurs primarily at night, when  
46 stomata are closed and the vapor pressure deficit (VPD) that typically drives transpiration is low,  
47 resulting in a greater water potential gradient among soil layers than between soil and the  
48 atmosphere (Oliveira et al. 2005b). HR has been observed and quantified in a variety of ecosystems  
49 across the world and has been shown to increase water and nutrient availability in shallow soils  
50 (Priyadarshini et al. 2015). Soil water availability ultimately affects nutrient uptake and whole  
51 plant carbon assimilation. Species with access to deeper groundwater may exhibit increased whole-  
52 plant drought resistance, and HR likely provides other physiological advantages (Nadezhdina et  
53 al. 2010, Neumann and Cardon 2012, David et al. 2013). For example, consistent water availability  
54 maintained via HR increases the lifespan of shallow fine roots, ensuring these species can take  
55 advantage of rainfall pulses following drought (Bauerle et al. 2008). Additionally, HR can increase  
56 diffusion rates of nutrients within the soil, which facilitates nutrient uptake and biotic soil  
57 processes during periods of low precipitation (Nippert and Knapp 2007, Scott et al. 2008b).  
58 Despite the importance of HR in forest ecosystems, relatively little is understood about  
59 interspecific variation in the timing and magnitude of HR in forests with distinct water resources

60           Measurements of nocturnal sap flux among co-occurring species in different forests  
61 systems suggest that rooting profile and water transport capacity influence HR (Scholz et al. 2008,  
62 Neumann and Cardon 2012). Rooting profile here is a multi-dimensional term referring to a tree's  
63 gross rooting depth, rooting distribution, and root morphology across that distribution. There is a  
64 great deal of evidence for environmentally controlled plasticity in rooting morphology, but broad  
65 differences in rooting profiles remain among distally related taxa (Callaway, 1990; Canadell, J., et

66 al., 1996; Jackson, R. B., et al., 1996; Hipondoka & Versfeld, 2006). Morphological differences  
67 in pine and oak rooting systems have been observed at coarse and fine scales, at all stages of  
68 growth (Comas et al., 2002; Curt et al., 2005; Kono<sup>^</sup>pka et al., 2005). When species with distinct  
69 rooting profiles are co-occurring in an ecosystem, the ability to transport water as nocturnal HR  
70 will differ among them. In the Cerrado savannas, tree species that rely exclusively on either  
71 shallow or deeper soil water have a poor capacity for HR in contrast to those that bridge across  
72 multiple soil strata (Scholz et al. 2008). In the coastal plain sandhills of the southeastern US, *Pinus*  
73 and *Quercus* species are known to redistribute groundwater, but the reported magnitudes of  
74 redistribution are inconsistent (Espeleta et al. 2004, Domec et al. 2010). These inconsistencies in  
75 magnitude could be the result of differences in measurement techniques among studies, such as  
76 psychrometry and sap flux, or due to differences in site-specific hydrology. Despite this, HR has  
77 been observed more frequently in *Pinus* species than co-occurring hardwoods of the southeastern  
78 US, potentially due to higher plasticity in their rooting morphology, but the mechanism remains  
79 unclear (Espeleta et al. 2004). These interspecific variations become especially important when  
80 accounting for HR as a function of an ecosystem's hydrologic budget. Redistributed water is often  
81 overlooked when assessing specific responses to water deficits, but can represent significant  
82 additions to shallow soil and whole-plant transpiration (Domec et al. 2010).

83         It has been hypothesized that species more readily redistributing water through their  
84 rooting profile should have an advantage mitigating water stress within shallow lateral roots during  
85 periods of drought (Emerman and Dawson 1996, Amenu and Kumar 2008); however, this has yet  
86 to be shown in an empirical study. In addition to considering differences in rooting morphology,  
87 it is necessary to understand the degree to which tree species are capable of drawing from deeper  
88 groundwater to supplement low moisture content of shallow soils (Ehleringer and Dawson 1992).

89 Water from different soil strata can be used as a source for both HR and transpiration demand  
90 (Scott et al. 2008a). HR of deep groundwater has been observed up to a depth of 20m across arid  
91 regions of central Texas (Bleby et al. 2010). If a species does not have access to deeper  
92 groundwater, it may show a reduced HR capacity, or it may transfer water laterally from wetter  
93 soils to drier soils, rather than mixing soil water between strata (Scholz et al. 2008). For example,  
94 in the Amazon Basin, despite a water table more than 100m deep, HR can still occur across shallow  
95 soil and non-saturated soil layers between 6 – 11m (Oliveira et al. 2005a). This indicates HR may  
96 only be limited by the heterogeneity of water availability across a plant's rooting profile, rather  
97 than depth to saturated soils (Kembel and Cahill 2005).

98         Understanding how environmental factors that influence tree transpiration also influence  
99 HR could facilitate a mechanistic understanding of HR, thereby providing a framework for  
100 predicting HR dynamics from commonly measured variables (Richards and Caldwell 1987a,  
101 Burgess et al. 1998). It is predicted that the highest rates of HR occur during periods of low shallow  
102 soil moisture (Neumann and Cardon 2012). This assumes water potential differences among soil  
103 strata are the primary driver of HR, and not the strength of the gradient among soil, plant, and  
104 atmosphere (Emerman and Dawson 1996). However, it has also been hypothesized that extremely  
105 low soil moisture may hinder HR capacity due to the high rate of fine root mortality (Wang et al.  
106 2011). High nocturnal VPD has also been linked to nocturnal transpiration in many plant species  
107 (Dawson et al. 2007), which may depress HR capacity as the atmosphere competes as a strong  
108 driver for water loss through stomata. To eliminate the confounding effect of nocturnal  
109 transpiration on HR, VPD must consistently reach zero at night, reducing the competition between  
110 atmosphere and soil water gradients (Dawson et al. 2007).

111 Using a xeric longleaf pine (Family-Pinaceae, *Pinus palustris* Mill.) woodland, we explore  
112 the capacity, interspecific variation, and water source of HR among dominant overstory conifer  
113 (*P. palustris*) and ring-porous hardwood trees (*Quercus laevis* Walter and *Q. margarettae* Ashe;  
114 Fagaceae). Our first objective was to quantify the volume and rate of water replacement during  
115 nocturnal HR for each of our study species. For this study, we constrain our use of HR and related  
116 terminology to the movement of water solely within plant tissues, not across the root-to-soil  
117 interface. We expected *P. palustris* to have a higher capacity for HR per unit area than either  
118 *Quercus* species, due to its heavy carbon investment in belowground rooting biomass (Brockway  
119 and Outcalt 2000). The second objective was to identify the water resources accessible to these  
120 tree species by determining the source of HR water. Longleaf pine woodlands of southwest  
121 Georgia have high annual precipitation, high daily VPD and consistently low nocturnal VPD (Ford  
122 et al. 2008). The xeric woodland where this study occurred has deep, sandy, excessively well-  
123 drained soils resting atop a thinly confined karst-limestone aquifer (Bosch et al. 2003, Williams  
124 and Kuniansky 2016). We expected species with access to deeper ground water to show no  
125 relationship between shallow soil moisture and transpiration within their main stem. Finally, to  
126 determine if environmental factors could predict observed patterns in HR, we correlated the  
127 magnitude of observed HR to temperature, VPD, and soil moisture.

## 128 **Methods**

### 129 *-Site Description-*

130 We conducted this study at the Jones Center at Ichauway, a privately-owned research site  
131 of 11,400 ha in the Dougherty Plain physiological district of southwest Georgia, USA. The climate  
132 is classified as humid subtropical, with ~1310 mm mean annual precipitation and 19 °C mean  
133 annual temperature. This region sits atop the Upper Floridan Aquifer (UFA) at one of its closest

134 points to the surface with a minimal confining unit. The UFA is an open, water-filled karst cavern  
135 system, which feeds directly into many of the surrounding river and stream systems and relies on  
136 soil filtration for recharge (Williams and Kuniansky 2016).

137 Our site was located in xeric soils (Goebel et al. 1997) immediately adjacent to the  
138 Ichawaynochaway Creek. The site occupies a flat plateau, approximately 10 m above the creek,  
139 with porous, excessively well-drained sandy soil that supports low volumetric water content (mean  
140 < 6% VWC). We selected four individuals from three dominant canopy tree species: *P. palustris*  
141 (mean DBH 32.15cm), *Q. laevis* (mean DBH 28.01cm), and *Q. margarettae* (mean DBH  
142 27.75cm), with *P. palustris* occurring across a broad range of soil types and the latter two species  
143 primarily associated with xeric sites. During the study period (June-November), 615 mm of rainfall  
144 were recorded at a nearby USGS rain gauge (USGS gauge #02355350). There was a period of low  
145 rainfall beginning in mid-September until the end of the study in November, less than 10% of the  
146 total recorded precipitation was observed in that time period. Mean daily temperature ranged from  
147 8 C° - 28 C°, with a mean of 23.9 C°. We recorded soil moisture at 20 cm depth (EC-5cm, METER,  
148 Pullman, Washington, USA) in 15-minute intervals throughout the duration of the study.

#### 149 -Sap flux-

150 We constructed heat ratio method (HRM) sap flux sensors following the Burgess et., al  
151 (2001) methodology. The HRM utilizes an upstream and downstream thermocouple with a central  
152 heat pulse to allow for bi-directional sap flux measurements. The accuracy of these sensors excels  
153 at low to medium flow conditions (Steppe et al. 2010). These two properties make the HRM ideal  
154 for capturing flow during nocturnal HR and contrasting against diurnal water uptake. For each  
155 tree, we installed two HRM sensors in opposing lateral roots 30cm from the stem base and an

156 additional sensor in each primary stem at a height of 1.3m to estimate total tree transpiration.  
157 Aluminum templates were used to install HRM sensors in a -1cm, 0cm, 1cm configuration for both  
158 root and main stem sensors (Burgess et al. 2001).

159 Dataloggers (CR1000, Campbell Scientific, Logan, Utah, USA) recorded thermocouple  
160 temperature for 80 s after a 6 s heat pulse, every 30 minutes. To determine sap velocity ( $V_s$   $cm\ sec^{-1}$ )  
161  $^l$ ), we first calculated heat pulse velocity ( $V_h$   $cm\ sec^{-1}$ ) from thermocouples and applied to the  
162 equation:

$$163 \quad V_h = \left(\frac{k}{x}\right) * \ln\left(\frac{v_1}{v_2}\right) * 3600$$

164 where  $k$  is the thermal diffusivity constant ( $Wm \cdot K^{-1}$ ),  $x$  is distance between heating element  
165 and sensor, and  $v_1$  and  $v_2$  denote the thermocouple temperatures after the heat pulse (Burgess et al.  
166 2001). To calculate  $k$ , we weighed and oven dried sapwood samples from each species to obtain  
167 density and water content. From there, we solved equations for the true calculation of  $k$  (Table 2.1)  
168 as outlined in Burgess et al. (2001).

169 The distance ( $x$ ) between heat pulse generation and thermocouple measurement is critical  
170 to calculating the heat pulse velocity, so error due to probe misalignment is a serious concern when  
171 using the HRM (Ren et al. 2017). To address this, we performed a two-week laboratory trial under  
172 zero flow conditions using four sensors in excised stem segments of each study species. We  
173 established these conditions by sealing both ends and the sensor installation points with silicone  
174 gel. The error due to probe misalignment during installation was calculated at less than 1% among  
175 all species. We applied this empirically derived error rate to the corrected heat pulse equations  
176 from Burgess et al. (2001):

177 
$$V_c = 4kt * \ln\left(\frac{v_1}{v_2}\right) - \frac{(x_1^2 - x_2^2)}{2t(x_1 - x_2)} * 3600$$

178

179 From the corrected heat pulse velocity ( $V_c$  *cm sec<sup>-1</sup>*),  $V_s$  can be calculated once wounding  
 180 effects are taken into account, based on sensor needle size and spacing.  $x_1$  is assumed to be the  
 181 correctly aligned distance between the thermocouple and heat pulse, while  $x_2$  is the incorrectly  
 182 aligned distance based on the two-week laboratory trial. The  $t$  variable connotes the time (sec)  
 183 between heat pulses. Afterwards, the final sap velocity was calculated using the corrected heat  
 184 pulse value:

185 
$$V_s = \frac{V_c \rho_b (c_w + m_c c_s)}{\rho_s c_s}$$

186 where  $\rho_b$  ( $\text{g cm}^{-3}$ ) denotes the density of wood,  $c_w$  and  $c_s$  ( $\text{J g}^{-1} \text{ }^\circ\text{C}$ ) denote the specific heat  
 187 capacity of the wood and sap respectively,  $m_c$  denotes the water content of sapwood ( $\text{ml g}^{-1}$ ), and  
 188  $\rho_s$  ( $\text{g cm}^{-3}$ ) denotes the density of water (Burgess et al. 2001). Positive sap velocity indicated uptake  
 189 due to transpiration, while negative sap velocity indicated reverse sap flux, which we attribute to  
 190 nocturnal HR transport out of lateral roots.

191 *-Conductive Sapwood Area-*

192 For each study species, we estimated conductive sapwood area (CSA) via active staining  
 193 of stem and root tissues (Reyes-García et al. 2012). Before peak transpiration ( $\sim 9$  am), a 1-cm  
 194 diameter hole was drilled into each tree at a height of 1.3m, or at 30cm from the tree base for root  
 195 samples. We drilled these holes either to a depth of half the stem diameter or 15cm (whichever  
 196 was lower), and gravity-fed crystal violet dye into the drill hole. We sampled from trees adjacent  
 197 to the sample flow site with a DBH range for *P. palustris* ( $n = 17$ ) between 5.3 cm to 28.2 cm, *Q.*  
 198 *laevis* ( $n = 13$ ) between 4.8 cm to 31.4 cm, and *Q. margarettae* ( $n = 10$ ) between 4.0 and 35.5 cm.

199 After 24 hours, wood bore samples 3 cm above the drilled hole, and the length of stained tissue  
200 were measured. We calculated conductive sapwood area from the stained tissue via:

$$201 \quad A_{sw} = \pi * \left( \left( \frac{D_t}{2} \right) - L_b \right)^2 - \left( \left( \frac{D_t}{2} \right) - L_{sw} - L_b \right)^2$$

202  
203 where  $A_{sw}$  is the CSA,  $D_t$  is the total diameter,  $L_b$  is the bark depth, and  $L_{sw}$  is the measured  
204 sapwood depth from the crystal violet stain.

205 *-Stable Isotope Analysis-*

206 We analyzed precipitation water, soil water, and water from plant xylem for analysis of  
207  $\delta^{18}\text{O}$  and  $\delta\text{D}$  isotope ratios in August and October 2017 to capture variations under different soil  
208 moisture conditions. We obtained soil water samples from 20 and 100 cm depths, and wood  
209 samples from the three study tree species (n = 10 per species). Deep soil pits were infeasible due  
210 to the risk of collapse in sandy soil, but a well water pump was available close to the site to collect  
211 deeper samples from > 10m underground (n = 10). Plant water samples were taken from the  
212 terminal ends of the lowest branches. We collected precipitation immediately prior to the October  
213 2017 collection. After collection, we wrapped sample vials in paraffin wax to prevent evaporation  
214 and immediately put them on ice for transport to the laboratory.

215 We cryogenically extracted plant and soil water from each sample at 155 °C for 25 minutes,  
216 verified to be within 99% of water extracted (Werner and Brand 2001). We then sent the samples  
217 to a stable isotope mass spectrometry lab, the UGA Center for Applied Isotope Studies, to obtain  
218  $\delta^{18}\text{O}$  and  $\delta\text{D}$  ratios.  $\delta^{18}\text{O}$  and  $\delta\text{D}$  were analyzed by sources (20 cm soil, 100 cm soil, and ground  
219 water) and mixtures (*P. palustris*, *Q. laevis*, and *Q. margarettae*).

220 -Environmental Drivers of HR-

221 To examine the relationship between stem and root sap flux and environmental factors, we  
222 obtained data from an array of environmental variables recorded within our study site using a  
223 HOBO weather station (ONSET, Bourne, Massachusetts). Our measured variables were 20 cm  
224 soil volumetric water content (VWC), mean daily vapor pressure deficit (VPD), maximum daily  
225 VPD, solar radiation, and mean nightly air temperature (Fig 5).

226 -Data Analyses-

227 We correlated CSA to DBH and created species specific allometric equations for *P.*  
228 *palustris* ( $y = 1.22e^{-0.044x}$ ;  $R^2 = 0.89$ ), *Q. laevis* ( $y = 1.403e^{-0.073x}$ ;  $R^2 = 0.97$ ), and *Q. margarettae*  
229 ( $y = 1.0874e^{-0.052x}$ ,  $R^2 = 0.97$ ). These equations were applied to a standard diameter for the lateral  
230 roots (5 cm) and main stem (25cm) to obtain CSA estimates for each species. Flow volumes were  
231 calculated using the velocity at each HRM sensor and multiplied by the species-specific CSA. We  
232 summed diurnal and nocturnal flow events separately to obtain hourly sap volumes to test for the  
233 effect of species on mean transpiration (diurnal sap flow) and HR (nocturnal sap flow) over the  
234 course of this study. We used these data in a mixed-effects repeated measures ANOVA with  
235 species as a fixed effect, time as the fixed repeated factor, and individual tree as the random effect.

236 We imposed stepwise regression based on minimum AIC to determine the environmental  
237 variables which explained a significant portion of HR variation. We analyzed the factors chosen  
238 above and their interactions against mean cumulative diurnal uptake and mean cumulative  
239 nocturnal HR for each species in a multivariate ANOVA. We plotted the predicted relationship  
240 from these tests against the observed data to determine how well these two factors could predict  
241 HR outflow.

242  $\delta^{18}\text{O}$  and  $\delta\text{D}$  ratios from soil sources and plant mixtures were plotted against the local  
243 meteoric water line (LMWL) for southwest GA, but were heavily fractionated (Jian Wang and  
244 Bojie 2019). Many of the plant sample values lay outside the boundary of the soil sources. To  
245 understand these outlying mixtures, we analyzed the source  $\delta^{18}\text{O}$  and  $\delta\text{D}$  contributions to the plant  
246 mixture ratios using a Bayesian stable isotope mixing model (SIMM) in R (iterations = 10000,  
247 burn rate = 1000, using statistical mean and standard deviation) (Parnell et al. 2013, Jian Wang  
248 and Bojie 2019).

## 249 -Results-

### 250 -Lateral Root Sap Movement-

251 *P. palustris* had the highest mean nocturnal HR in lateral roots ( $p < 0.001$ ) when compared  
252 to either *Quercus* species (Fig 1). Over the course of the study, mean ( $\pm\text{SE}$ ) lateral root uptake for  
253 *P. palustris* (6.2 cm mean diameter) was  $407.2 \pm 21.8 \text{ ml day}^{-1}$  (Fig 2). Less than 20% of uptake  
254 occurred during the latter half of the study, between September and November (Fig 1). The  
255 opposite trend was found for *P. palustris*' mean nocturnal root outflow, estimated at  $198.1 \pm 18.1$   
256  $\text{ml day}^{-1}$ , 48% of root uptake. Over 50% of nocturnal HR in lateral roots occurred during the last  
257 two months of the study, between October and November (Fig 1).

258 *Q. margarettae* showed significantly higher mean HR than *Q. laevis* within the lateral roots  
259 ( $p = 0.003$ ). Mean lateral root uptake for *Q. margarettae* (6.1 cm mean diameter) was  $141.5 \pm 5.68$   
260  $\text{ml day}^{-1}$  (Fig 2) with a nocturnal root HR of  $89.1 \pm 9.7 \text{ ml}$ , 53% of root uptake. Mean lateral root  
261 uptake for *Q. laevis* (6.1 cm mean diameter) was  $81.6 \pm 2.656 \text{ ml day}^{-1}$  (Fig 2) with a root HR of  
262  $17.2 \pm 1.72 \text{ ml day}^{-1}$ , 21% of root uptake. The majority of HR ( $> 60\%$ ) for both *Quercus* species  
263 occurred between October and November (Fig 1).

### 264 -Main Stem Sap Movement-

265 *P. palustris* exhibited consistent fluctuations in stem uptake over the 158-day study. Mean  
266 diurnal uptake for the mean stem diameter (32.15 cm) was  $15.9 \pm 0.459$  L, significantly higher  
267 than either *Quercus* species ( $p < 0.001$ ). Mean main stem-mediated HR was  $10.2 \pm .680$  L, or 64%  
268 of uptake (Fig 2). More than 60% of stem-mediated HR occurred between October and November  
269 (Fig 1). *Q. laevis* exhibited a lower mean HR in the main stem than the other species ( $p < 0.001$ ).  
270 Mean uptake for the main stem diameter (mean = 28.75 cm) was  $8.09 \pm 0.301$  L day<sup>-1</sup>. Mean main  
271 stem HR was  $1.99 \pm 0.219$  L day<sup>-1</sup>, or 25% of uptake (Fig 2). *Q. margarettae* had significantly  
272 greater mean daily stem-mediated HR than *Q. laevis* ( $p < 0.001$ ), but significantly lower HR than  
273 *P. palustris* ( $p < 0.001$ ). *Quercus laevis* exhibited an increased stem uptake during the last two  
274 months, October through November, which accounted for over 40% of total water use during the  
275 study (Fig 1). Mean uptake for the main stem (mean diameter 27.40 cm) was  $5.53 \pm 0.395$  L day<sup>-1</sup>.  
276 HR within the main stem was less consistent and accounted for a smaller proportion of daily  
277 uptake than was observed in lateral roots. Mean daily main stem HR was  $2.17 \pm 0.223$  L, 39% of  
278 uptake (Fig 2). Similar to *Q. laevis*, the majority of HR (>60%) within the main stem occurred  
279 between October through November (Fig 1).

#### 280 -Stable Isotope Analysis-

281 Source water usage was similar among species during a period of high VWC in August,  
282 but differed among species during an extended period of low VWC in October (Fig 3). In August,  
283 *P. palustris* received an estimated mean ( $\pm$ SE) source contribution of  $4.75 \pm 1.24\%$  of water from  
284 20 cm soil layer,  $6.95 \pm 2.05\%$  of water from the 100 cm deep soil layer, and  $88.3 \pm 2.59\%$  of  
285 water from groundwater (Fig 3). These proportions were closely matched by *Q. laevis* ( $5.61 \pm$   
286  $1.41\%$ ,  $7.67 \pm 2.10\%$ , and  $86.7 \pm 2.71\%$  respectively) and *Q. margarettae* in August ( $5.92 \pm 1.23\%$ ,  
287  $6.85 \pm 1.53\%$ , and  $87.2 \pm 1.91\%$ , respectively) (Fig 3). The October samples show different water

288 sources within all three study species. *P. palustris* was estimated to source  $32.4 \pm 6.0\%$  of xylem  
289 water from 20 cm soil layer,  $38.8 \pm 7.22\%$  of xylem water from the 100 cm deep soil layer, and  
290  $28.8 \pm 5.38\%$  of xylem water from groundwater in October (Fig 3). These proportions were similar  
291 in *Q. laevis* ( $35.2 \pm 6.41\%$ ,  $40.7 \pm 7.5\%$ , and  $24.1 \pm 4.87\%$  respectively), but differed substantially  
292 in *Q. margarettae* ( $68.8 \pm 6.42\%$ ,  $20.4 \pm 5.69\%$ , and  $10.8 \pm 2.76\%$ , respectively). (Fig 3).

### 293 -Environmental Drivers of HR-

294 For all species, mean daily uptake had a moderate to strong positive relationship with mean  
295 daily VPD (mean *P. palustris*  $R^2 = 0.56$ ; *Q. laevis*  $R^2 = 0.73$ ; *Q. margarettae*  $R^2 = 0.49$ ). When  
296 relating HR to environmental factors, all three species showed a moderate to strong relationship  
297 between HR and the combination of nightly air temperature, mean daily VPD (kPa), and their  
298 interactive effects (*P. palustris*  $R^2 = 0.71$ ; *Q. laevis*  $R^2 = 0.85$ ; *Q. margarettae*  $R^2 = 0.90$ ). Mean  
299 nightly temperature ( $^{\circ}\text{C}$ ) explained 64% of the variation in HR for *P. palustris*, 68% for *Q. laevis*,  
300 and 78% for *Q. margarettae* (Table 2). This was an inverse relationship with HR, increasing HR  
301 as mean temperature decreased. By contrast, mean daily VPD (kPa) only explained 2 – 14% of the  
302 daily variation in HR among all three species (Table 2). Daily VPD (kPa) had a positive  
303 relationship with HR. Most surprisingly, hourly soil VWC did not explain enough variation in  
304 mean nocturnal HR to be included in any regression models (Table 2).

### 305 -Discussion-

306 Based on our estimates, HR in the lateral roots for *P. palustris* equaled almost half of the  
307 volume used for transpiration (Fig 2). The magnitude of HR in the lateral roots was significantly  
308 higher in *P. palustris* and *Q. margarettae* than what was found in *Q. laevis*. We found that all three  
309 species were capable of water uptake from multiple soil strata, and that the reliance upon these  
310 strata was not constant throughout the study period (Fig 3). The environmental factors we

311 considered (VPD, soil moisture, and temperature) explained much less variation in HR than  
312 predicted. Temperature had the strongest impact on HR volumes, showing increased prevalence  
313 and magnitude of HR as temperatures cooled during the months of October and November (Table  
314 2). Temperature and VPD have a strong co-variation and are typically not used as separate factors  
315 when assessing relationships with transpiration. However, for HR, these factors appear to have  
316 differing influence, suggesting a de-coupling of temperature and VPD as it relates to nocturnal HR  
317 fluxes. Additionally, temperature at our site was variable during peak HR, while hourly VPD  
318 reached zero for 87% of the nights during this study.

319 *P. palustris* exhibited higher volumes of HR through lateral roots and main stem than either  
320 *Quercus* species, despite similarities in numbers of lateral roots and sap velocities (Dupuy et al.  
321 2005a). The higher cross-sectional sapwood area (CSA) in *P. palustris* contributed to greater water  
322 use and HR as compared to either *Quercus* species. This was seen primarily in the main stem,  
323 which had more than double the mean daily transpiration of either *Quercus* species (Fig 2). The  
324 lateral roots of *Q. margarettae* had significantly higher water use than *Q. laevis*, suggesting it may  
325 be more reliant on its lateral root system for water acquisition than the main tap root. Their lateral  
326 roots seem to be able to access water from a variety of soil strata, an idea supported by water source  
327 estimates during August and October 2017 (Fig 3). *Q. laevis* by contrast had significantly lower  
328 mean daily water uptake within the lateral roots, but a higher overall uptake in the main stem (Fig  
329 2). If *Q. laevis* was more reliant on a deep-water source, it would agree with the isotope data  
330 indicating that it relied less on shallow soil water than *Q. margarettae* during times of higher  
331 shallow soil moisture availability (Fig 3).

332 The  $\delta^{18}\text{O}$  and  $\delta\text{D}$  within xylem tissue indicate all three species alter their reliance upon  
333 different soil strata for water uptake (Fig 3), likely in response to changes in water potential

334 gradients (Dawson and Pate 1996). During the August collection, shallow soil VWC was at a low  
335 for the month (~3%); however, in October the collection occurred immediately after the largest  
336 rain event of the month when shallow-soil VWC was recorded at 6.4%, which is quite high for this  
337 site. This suggests these tree species, like many other plants, utilize soil water from the source of  
338 highest water potential, or strongest gradient between soil and atmosphere. Of all species, *Q.*  
339 *margarettae* showed the strongest shift between groundwater and shallow water sources,  
340 indicating that it may devote more resources to root biomass in the upper 20cm of the soil profile,  
341 and still maintain a tap root deep enough to capitalize on groundwater (Fig 3). All three species  
342 preferentially uptake shallow soil water when available, but the isotope data suggest some portion  
343 of water is always sourced from groundwater (Fig 3).

344         We predicted that *P. palustris* would be better able to access ground water and thus, rely  
345 more heavily upon this resource than either *Quercus* species due to early-life root development  
346 and larger tap-root morphology (Barnett, 2002). If these species show a strong morphological  
347 difference, it would be expected to display itself among their hydrological niche differentiation  
348 (Nippert and Holdo 2015), preferentially using the groundwater resource that other species have  
349 difficulty accessing. However, the inference from our water partitioning data suggest that all three  
350 of these species acquired water from similar sources. Shallow soil VWC (i.e., 20cm) was not  
351 correlated with diurnal sap flow, indicating the de-coupling between shallow soil water and  
352 transpiration that occurs if species have access to groundwater. Moreover, the two *Quercus* species  
353 showed the greatest difference between water sources during both August and October potentially  
354 indicating hydrologic differentiation is occurring more strongly between the more closely related  
355 species.

356 A factor potentially influencing the source contributions of water in our study was the  
357 effect of HR itself on the isotopic ratios of shallow soil water via mixing of distinct isotope N  
358 members. We hypothesize, due to the high volume of HR in this system, that there may be a  
359 dampening effect which artificially lowers the  $\delta^{18}\text{O}$  and  $\delta\text{D}$  of shallow soil water. This would affect  
360 the baseline comparisons that were used in our model, causing less discrimination among soil  
361 strata, and appearing as a more “well mixed” system. Tree species would be observed to rely on  
362 more varied sources of soil water than in reality. Several previous studies have used labeled  $\delta\text{D}$   
363 tracers to confirm the presence of HR in shallow soils across a variety of ecosystems (Brooks et  
364 al. 2002, Leffler et al. 2005, Priyadarshini et al. 2016). This methodology acknowledges the  
365 vertical mixing of soil water that occurs due to HR, made apparent by deuterated water’s extreme  
366  $\delta\text{D}$ . It is unclear to what degree HR may confound the natural  $\delta^{18}\text{O}$  and  $\delta\text{D}$  gradients that would  
367 otherwise be present. Future studies may need to rely on distinctly labeled water tracers, injected  
368 across the rooting profile, to determine tree water sources without the influence of HR mixing.

369 The large proportion of negative flow events recorded in the main stem of all three species  
370 lends more evidence to the stem-mediated HR hypothesis (Burgess and Bleby 2010). Because  
371 these three species all have a tap root with a pattern of access to deeper soil strata, it is likely that  
372 water transported via HR must first travel within the main stem before exiting through the lateral  
373 roots. Stem-mediated HR as observed in this study is useful in relating total daily transpiration to  
374 HR but could only be used as a conservative estimate if lateral root data were not available. As has  
375 been shown in other studies, roots provide the most accurate estimates of HR, as stem-mediated  
376 HR is only a portion of total tree HR and the magnitude is very sensitive to changes in both sensor  
377 height and azimuth (Burgess and Bleby 2006, Nadezhdina et al. 2009). Our stem-mediated HR  
378 estimates match well with the magnitude of HR in the lateral roots, averaging between three to

379 seven times greater than major individual lateral roots. These numbers agree well with the number  
380 of major lateral roots estimated in these species by past research (Drexhage et al. 1999, Dupuy et  
381 al. 2005b).

382 The consistency of HR changed throughout the study with higher magnitudes during  
383 October and November (Fig 1). Temperature had an inverse relationship with HR (Table 2), with  
384 each species having an increase in HR during cooler periods. Colder months typically result in  
385 lower mean carbon assimilation for both *Quercus* and *Pinus* species (Law et al. 1999). If leaves  
386 are senescing or closing their stomata more frequently, it may allow for daytime HR to occur as  
387 VPD is no longer a driving force on xylem water transport (Leffler et al. 2005, Gou and Miller  
388 2014). Mean daily VPD was a weak predictor of mean daily HR for each species, which agrees  
389 with our current understanding, since HR movement primarily occurs at night, when VPD is  
390 typically zero at our study site (Table 2).

391 Soil moisture (VWC) was a poor predictor of HR within the lateral roots of all study  
392 species. The relationship between soil moisture and HR has been clearly documented in prior  
393 research, but this specific system does not show as strong of a link (Scott et al. 2008a, Neumann  
394 and Cardon 2012). A difference of 7% VWC between the wettest and driest conditions may not be  
395 large enough to have an impact on HR's water movement. Rather, it may be that the difference  
396 between soil water content between strata is very large in the *P. palustris* woodlands due to  
397 excessively well-drained shallow soils sitting atop deeper, saturated soils and water-filled karst  
398 topography. According to the isotopic data, all three tree species appear to have access to deeper  
399 groundwater, which may have created a soil water potential gradient between shallow and deeper  
400 soils to drive HR regardless of fluctuations in shallow soil moisture conditions (Gou and Miller  
401 2014).

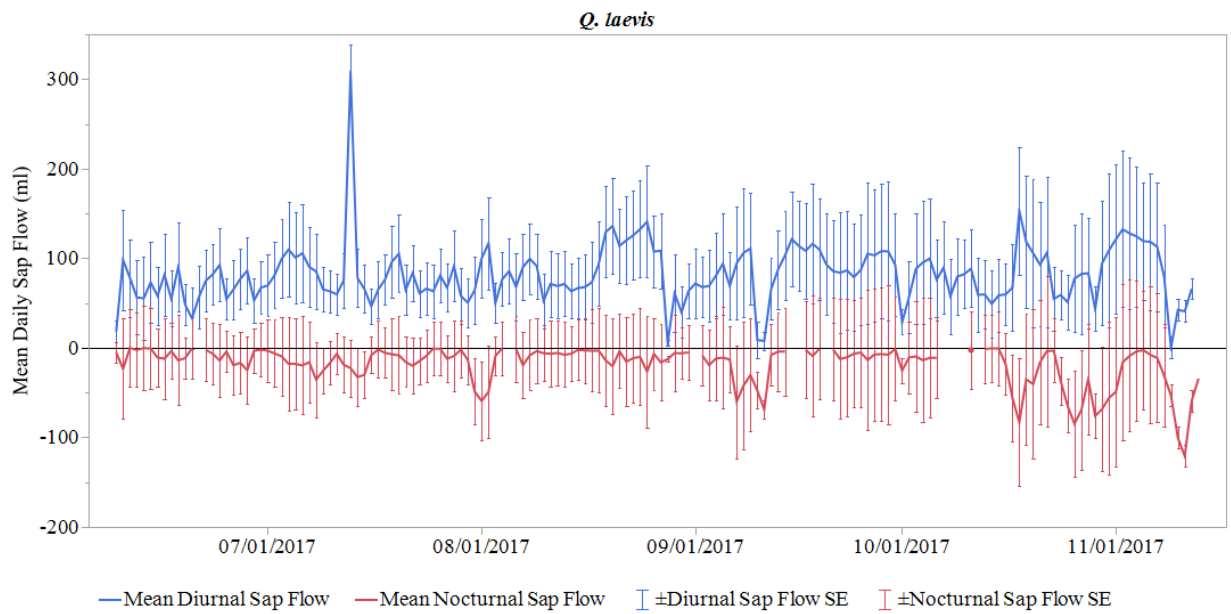
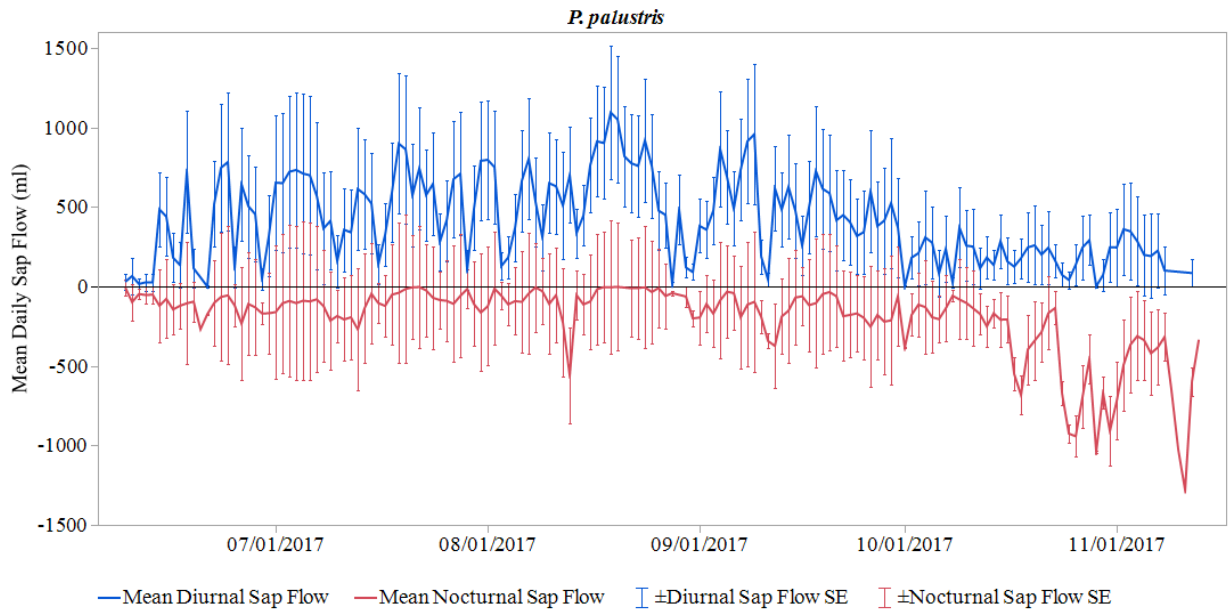
402           Our results suggest a substantial amount of water is transported during nocturnal HR and  
403 sourced from deeper groundwater. This deeper stratum is more saturated than shallow soils and  
404 linked to it by the rooting profile of all the three tree species studied here, but the highest  
405 magnitudes recorded in *P. palustris*. This connection allows the difference in soil moisture to drive  
406 HR upwards, redistributing both water and soil nutrients (Nadezhdina et al. 2010). This reasoning  
407 is often used to suggest that HR is able to act as a community level water subsidy for all taxa  
408 unable to otherwise access deeper groundwater (Muler et al. 2018). If this is the case, its role to  
409 facilitate mixed-tree grass systems needs to be quantified and incorporated into our current view  
410 of ecosystem water dynamics. Further research focusing on understory plant communities will  
411 highlight this potential role of HR in adding water subsidies to woodland ecosystems.

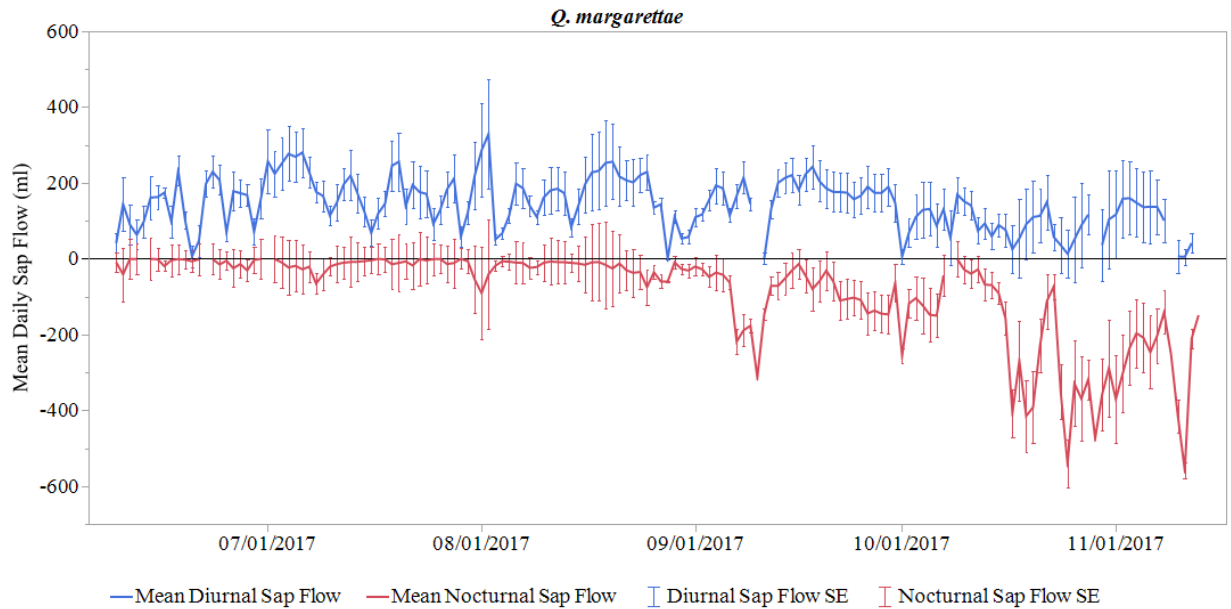
412 Acknowledgements

413 Funding was provided by the Robert W. Woodruff Foundation through the Jones Center at  
414 Ichauway. This material is based upon work supported by the Department of Energy under award  
415 number DE-EM0004391 to the University of Georgia Research Foundation. We would like to  
416 thank Stribling Stuber and Robert Ritger for assistance provided with data collection and logistics.  
417 For help with laboratory analyses, we would like to thank Seth Younger and the Jackson hydrology  
418 lab as well as the University of Georgia's Center for Applied Isotope Studies.

419 Table 1: Sap velocity constants for each study species. ( $k$  = thermal diffusivity ( $W(m \cdot K)^{-1}$ ),  $\rho_b$  =  
 420 density of wood,  $m_c$  = water content of sapwood ( $ml g^{-1}$ ),  $c_w$  = specific heat capacity of wood ( $J$   
 421  $g^{-1} C^\circ$ ))

	<i>P. palustris</i>	<i>Q. margarettae</i>	<i>Q. laevis</i>
$k$ ( $W(m \cdot K)^{-1}$ )	0.081	0.059	0.048
$\rho_b$ ( $g cm^{-3}$ )	0.42	0.77	0.71
$m_c$ ( $ml g^{-1}$ )	0.38	0.31	0.29
$c_w$ ( $J g^{-1} \text{ }^\circ C$ )	4.65	3.60	3.47

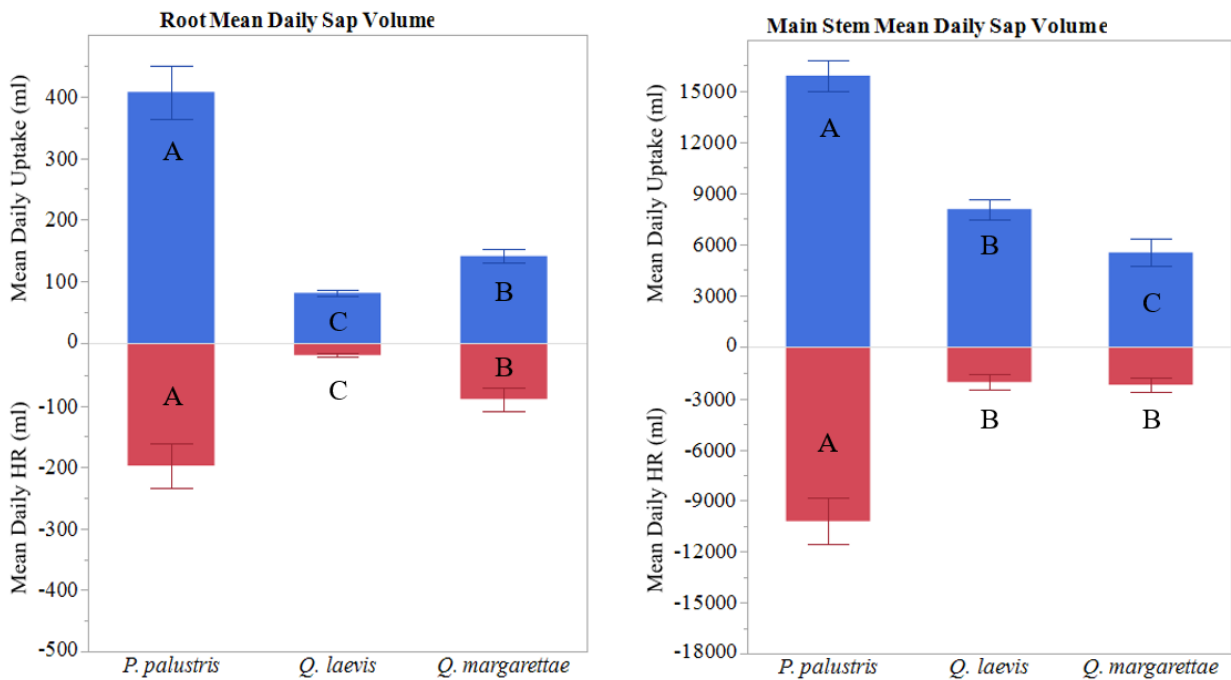




424

425

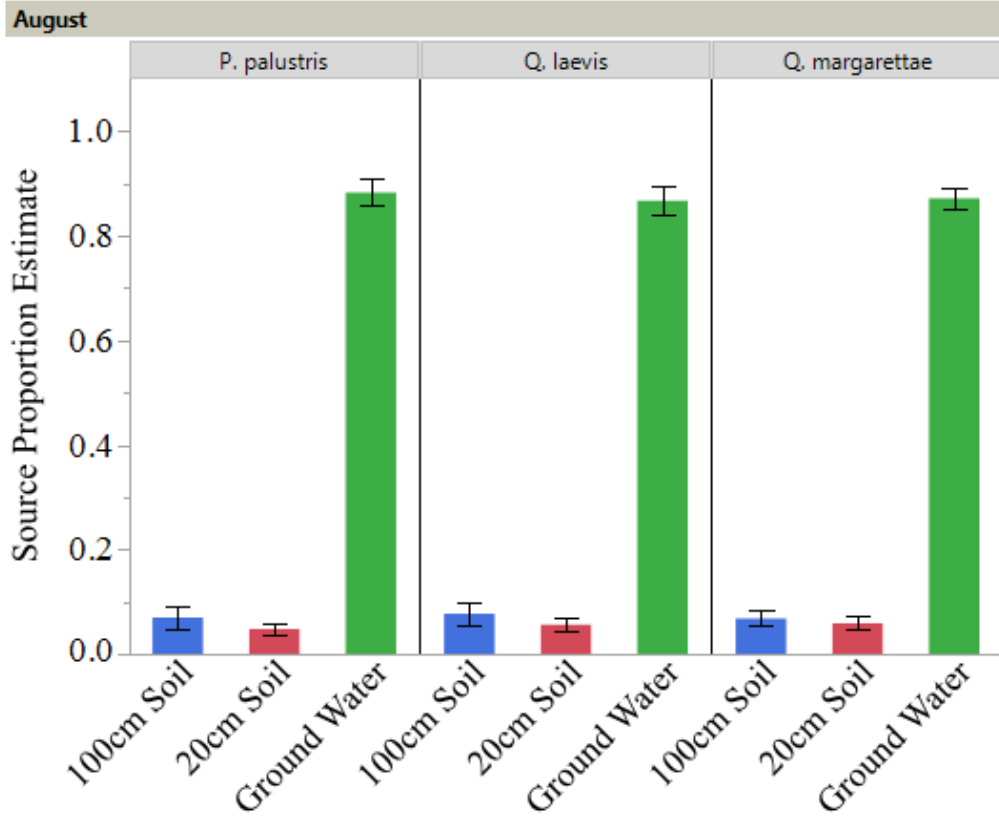
426 Figure 1: Mean daily uptake and HR in lateral roots among all three study species over the study  
 427 period. A large increase in HR is seen during the months of October and November, coinciding  
 428 with cooler temperatures and drier soil conditions.



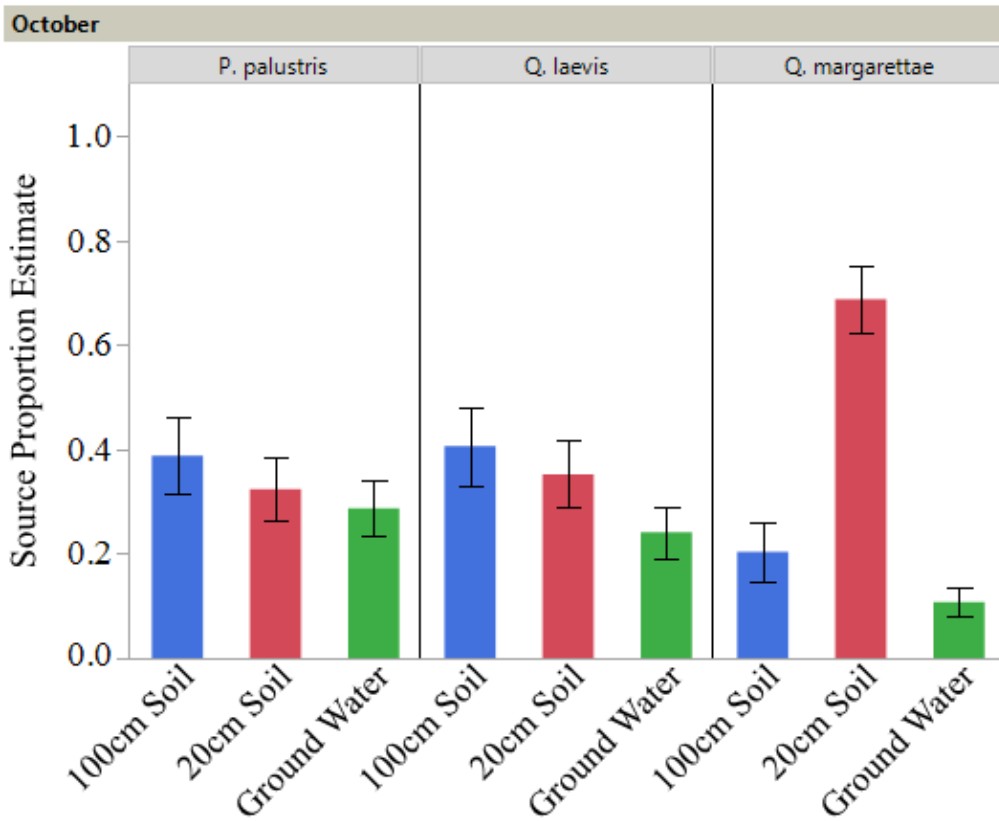
429

430 Figure 2: Comparison of mean diurnal uptake and nocturnal HR (ml) among species for lateral  
 431 roots and main stems, relativized for a 25cm DBH stem. Error bars represent the 95% confidence

432 interval around the mean and connecting letters indicate significant differences in uptake or HR  
433 among species based on Tukey HSD *post hoc* ( $\alpha = 0.05$ ).



434



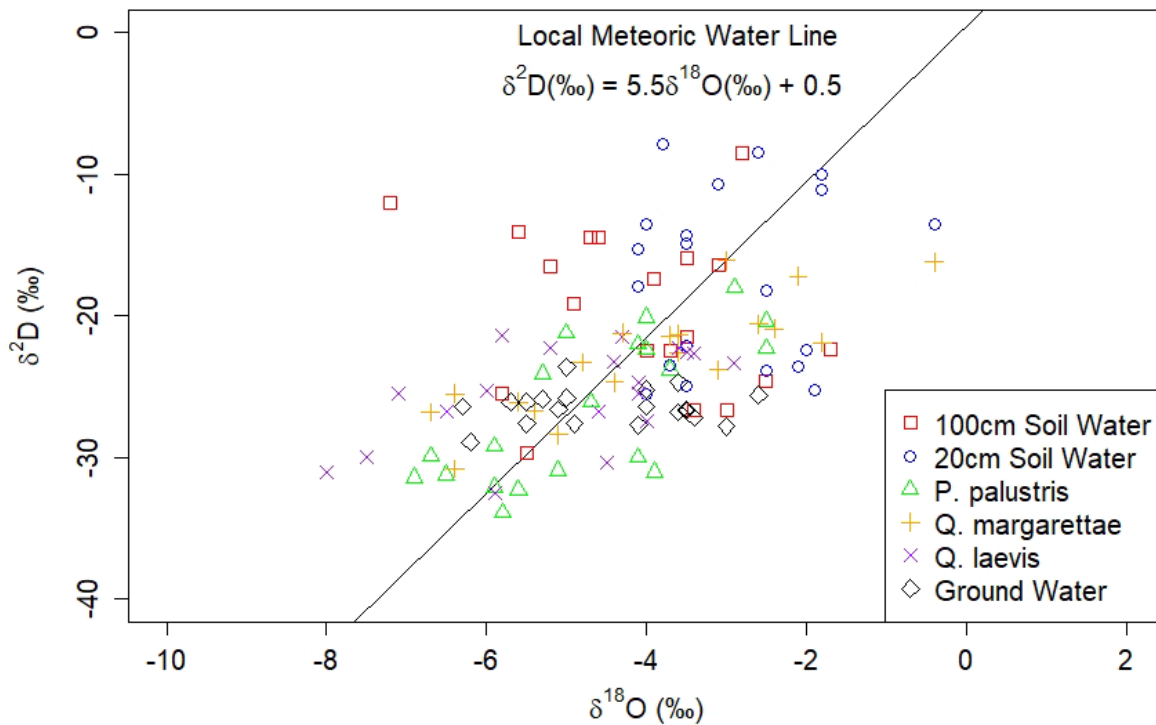
435

436 Figure 3: Comparison of estimated source contributions among *P. palustris*, *Q. laevis*, and *Q*  
437 *margarettae* xylem water samples during August and October 2017. Sources are: ground water,  
438 20 cm soil water, and 100 cm soil water. Error bars are constructed using standard error of the  
439 mean.

440 Table 2: Species models for the multiple regression analysis of mean daily HR. Factors were  
 441 selected via a stepwise regression based on minimum AIC. R<sup>2</sup> values are shown for the model as  
 442 well as the contributions for individual factors.

Species	AIC & Model Components	R <sup>2</sup>	Prob > F
<i>P. palustris</i>	Minimum AIC = 931.44	R <sup>2</sup> = 0.71	< 0.001
	Temperature	R <sup>2</sup> = 0.64	< 0.001
	Mean daily VPD	R <sup>2</sup> = 0.023	< 0.001
<i>Q. laevis</i>	Minimum AIC = 942.35	R <sup>2</sup> = 0.85	< 0.001
	Temperature	R <sup>2</sup> = 0.64	< 0.001
	Mean Daily VPD	R <sup>2</sup> = 0.13	< 0.001
	Temperature * Mean Daily VPD	R <sup>2</sup> = 0.021	0.004
<i>Q. margarettae</i>	Minimum AIC = 758.49	R <sup>2</sup> = 0.90	< 0.001
	Temperature	R <sup>2</sup> = 0.78	< 0.001
	Mean Daily VPD	R <sup>2</sup> = 0.14	0.0015

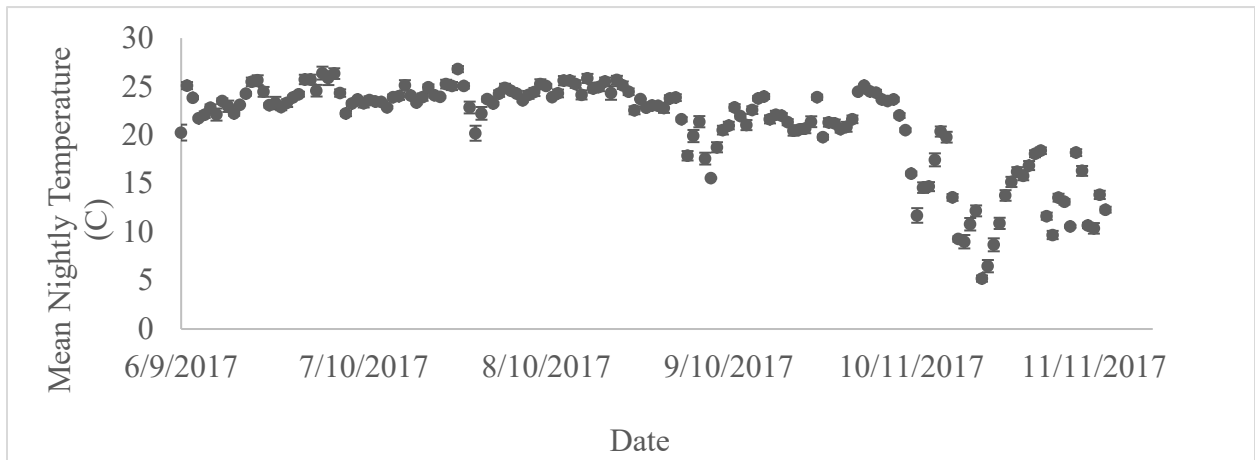
443



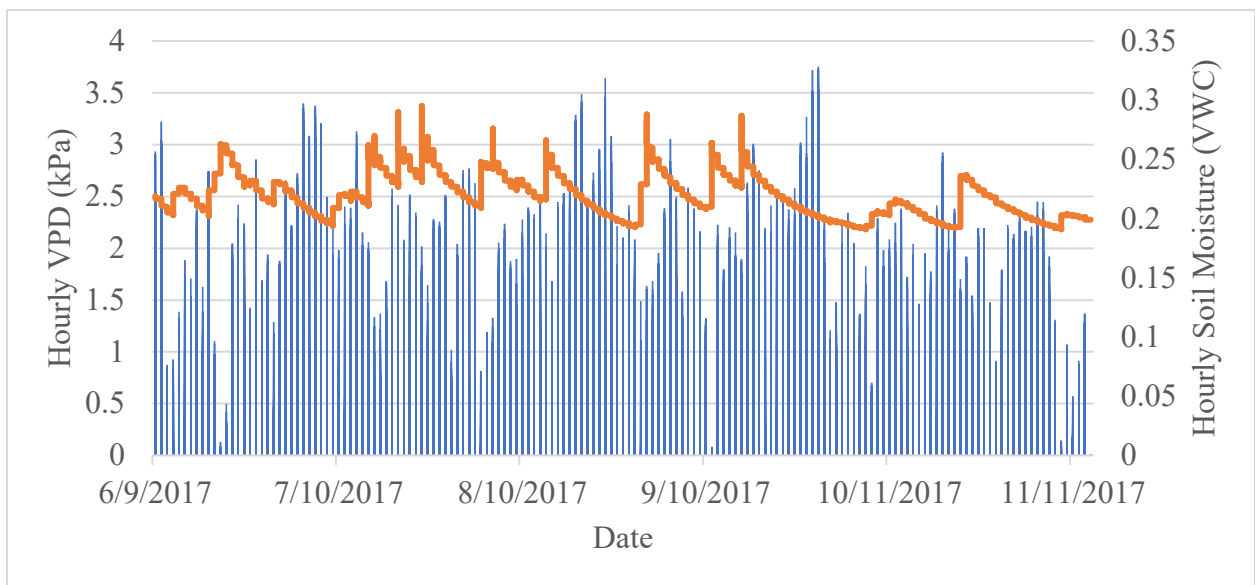
444

445 Figure 4: δ<sup>18</sup>O and δD isotope ratios for source and xylem water samples plotted against the local  
 446 meteoric water line (LMWL). The distribution of the points away from the LMWL indicates

447 preferential fractionation. Several xylem water mixtures lie beyond the range of our source  
448 samples indicating further fractionation. The Bayesian stable isotope mixing model was  
449 constructed from these ratios.



450  
451 (a)



452  
453 (b)

454 Figure 5: Raw nightly air temperature (a), mean daily VPD (b; blue bars), and hourly soil moisture  
455 (b; orange line) dataset used throughout the study period. These data contributed to the  
456 construction of our stepwise regression model relating HR to external environmental factors.

**Analysis of Variance**

Source	DF	Sum of Squares	Mean Square	F Ratio
Model	2	1670734	835367	126.4377
Error	1261	8331355	6607	<b>Prob &gt; F</b>
C. Total	1263	10002089		<b>&lt;.0001*</b>

**Parameter Estimates**

Term	Estimate	Std Error	t Ratio	Prob> t
Intercept	-234.4324	13.13098	-17.85	<b>&lt;.0001*</b>
VPD Mean	-32.79806	7.902156	-4.15	<b>&lt;.0001*</b>
Mean Temp	9.1437548	0.577636	15.83	<b>&lt;.0001*</b>

457

458 Supplemental Figure 1: Statistical output for *P. palustris* in our standard least squares model after  
 459 performing a stepwise regression to determine statistically relevant factors.

**Analysis of Variance**

Source	DF	Sum of Squares	Mean Square	F Ratio
Model	4	198453.04	49613.3	130.9007
Error	1259	477179.25	379.0	<b>Prob &gt; F</b>
C. Total	1263	675632.29		<b>&lt;.0001*</b>

**Parameter Estimates**

Term	Estimate	Std Error	t Ratio	Prob> t
Intercept	-81.66789	3.672271	-22.24	<b>&lt;.0001*</b>
Soil VWC	66.890829	40.33543	1.66	0.0975
VPD Mean	-12.95448	2.174927	-5.96	<b>&lt;.0001*</b>
Mean Temp	3.1610313	0.159287	19.84	<b>&lt;.0001*</b>
(VPD Mean-0.68649)*(Mean Temp-23.8911)	0.9595394	0.459472	2.09	<b>0.0370*</b>

460

461 Supplemental Figure 2: Statistical output for *Q. laevis* in our standard least squares model after  
 462 performing a stepwise regression to determine statistically relevant factors.

463

<b>Analysis of Variance</b>				
Source	DF	Sum of Squares	Mean Square	F Ratio
Model	2	197514.3	98757.2	59.9481
Error	1261	2077341.8	1647.4	<b>Prob &gt; F</b>
C. Total	1263	2274856.1		<.0001*

<b>Parameter Estimates</b>				
Term	Estimate	Std Error	t Ratio	Prob> t
Intercept	-87.4273	6.556819	-13.33	<.0001*
VPD Mean	-12.54051	3.945861	-3.18	0.0015*
Mean Temp	3.1516164	0.288437	10.93	<.0001*

464

465 Supplemental Figure 3: Statistical output for *Q. margarettae* in our standard least squares model  
 466 after performing a stepwise regression to determine statistically relevant factors.

467

468 **References**

- 469 Amenu, G. G., and P. Kumar. 2008. A model for hydraulic redistribution incorporating coupled  
470 soil-root moisture transport. *Hydrology and Earth System Sciences* **12**:55-74.
- 471 Bauerle, T. L., J. H. Richards, D. R. Smart, and D. M. Eissenstat. 2008. Importance of internal  
472 hydraulic redistribution for prolonging the lifespan of roots in dry soil. *Plant Cell and*  
473 *Environment* **31**:177-186.
- 474 Bleby, T. M., A. J. Mcelrone, and R. B. Jackson. 2010. Water uptake and hydraulic redistribution  
475 across large woody root systems to 20 m depth. *Plant, Cell & Environment* **33**:2132-2148.
- 476 Bosch, D. D., R. R. Lowrance, J. M. Sheridan, and R. G. Williams. 2003. Ground Water Storage  
477 Effect on Streamflow for a Southeastern Coastal Plain Watershed. *Ground Water* **41**:903-  
478 912.
- 479 Brockway, D. G., and K. W. Outcalt. 2000. Restoring longleaf pine wiregrass ecosystems::  
480 Hexazinone application enhances effects of prescribed fire. *Forest Ecology and*  
481 *Management* **137**:121-138.
- 482 Brooks, J. R., F. C. Meinzer, R. Coulombe, and J. Gregg. 2002. Hydraulic redistribution of soil water  
483 during summer drought in two contrasting Pacific Northwest coniferous forests. *Tree*  
484 *Physiology* **22**:1107-1117.
- 485 Burgess, S. S. O., M. A. Adams, N. C. Turner, C. R. Beverly, C. K. Ong, A. A. H. Khan, and T. M. Bleby.  
486 2001. An improved heat pulse method to measure low and reverse rates of sap flow in  
487 woody plants. *Tree Physiology* **21**:589-598.
- 488 Burgess, S. S. O., and T. M. Bleby. 2006. Redistribution of soil water by lateral roots mediated by  
489 stem tissues. *Journal of Experimental Botany* **57**:3283-3291.
- 490 Caldwell, M. M., T. E. Dawson, and J. H. Richards. 1998. Hydraulic lift: Consequences of water  
491 efflux from the roots of plants. *Oecologia* **113**:151-161.
- 492 Canadell, J., R. B. Jackson, J. B. Ehleringer, H. A. Mooney, O. E. Sala and E. D. Schulze (1996).  
493 "Maximum rooting depth of vegetation types at the global scale." *Oecologia* **108**(4): 583-  
494 595.
- 495 Comas, L., T. Bouma, and David Eissenstat. "Linking root traits to potential growth rate in six  
496 temperate tree species." *Oecologia* 132.1 (2002): 34-43.
- 497 Curt, Thomas, et al. "Plasticity in growth, biomass allocation and root morphology in beech  
498 seedlings as induced by irradiance and herbaceous competition." *Annals of Forest science*  
499 **62.1** (2005): 51-60.
- 500 David, T. S., C. A. Pinto, N. Nadezhdina, C. Kurz-Besson, M. O. Henriques, T. Quilhó, J. Cermak, M.  
501 M. Chaves, J. S. Pereira, and J. S. David. 2013. Root functioning, tree water use and  
502 hydraulic redistribution in *Quercus suber* trees: A modeling approach based on root sap  
503 flow. *Forest Ecology and Management* **307**:136-146.
- 504 Dawson, T. E., S. S. O. Burgess, K. P. Tu, R. S. Oliveira, L. S. Santiago, J. B. Fisher, K. A. Simonin, and  
505 A. R. Ambrose. 2007. Nighttime transpiration in woody plants from contrasting  
506 ecosystems. *Tree Physiology* **27**:561-575.
- 507 Dawson, T. E., and J. S. Pate. 1996. Seasonal water uptake and movement in root systems of  
508 Australian phraeatophytic plants of dimorphic root morphology: A stable isotope  
509 investigation. *Oecologia* **107**:13-20.

510 Domec, J. C., J. S. King, A. Noormets, E. Treasure, M. J. Gavazzi, G. Sun, and S. G. McNulty. 2010.  
511 Hydraulic redistribution of soil water by roots affects whole-stand evapotranspiration and  
512 net ecosystem carbon exchange. *New Phytol* **187**:171-183.

513 Drexhage, M., M. Chauviere, F. Colin, and C. N. N. Nielsen. 1999. Development of structural root  
514 architecture and allometry of *Quercus petraea*. *Canadian Journal of Forest Research-*  
515 *Revue Canadienne De Recherche Forestiere* **29**:600-608.

516 Dupuy, L., T. Fourcaud, and A. Stokes. 2005a. A Numerical Investigation into the Influence of Soil  
517 Type and Root Architecture on Tree Anchorage. *Plant and Soil* **278**:119-134.

518 Dupuy, L., T. Fourcaud, A. Stokes, and F. Danjon. 2005b. A density-based approach for the  
519 modelling of root architecture: application to Maritime pine (*Pinus pinaster* Ait.) root  
520 systems. *Journal of Theoretical Biology* **236**:323-334.

521 Ehleringer, J., and T. Dawson. 1992. Water uptake by plants: perspectives from stable isotope  
522 composition. *Plant, Cell & Environment* **15**:1073-1082.

523 Emerman, S. H., and T. E. Dawson. 1996. Hydraulic lift and its influence on the water content of  
524 the rhizosphere: An example from sugar maple, *Acer saccharum*. *Oecologia* **108**:273-278.

525 Espeleta, J. F., J. B. West, and L. A. Donovan. 2004. Species-specific patterns of hydraulic lift in co-  
526 occurring adult trees and grasses in a sandhill community. *Oecologia* **138**:341-349.

527 Ford, C. R., R. J. Mitchell, and R. O. Teskey. 2008. Water table depth affects productivity, water  
528 use, and the response to nitrogen addition in a savanna system. *Canadian Journal of*  
529 *Forest Research* **38**:2118-2127.

530 Goebel, P., B. Palik, L. Kirkman, and L. West. 1997. Field guide: landscape ecosystem types of  
531 Ichaaway. Newton, GA.

532 Gou, S., and G. Miller. 2014. A groundwater-soil-plant-atmosphere continuum approach for  
533 modelling water stress, uptake, and hydraulic redistribution in phreatophytic vegetation.  
534 *Ecohydrology* **7**:1029-1041.

535 Jackson, R. B., J. Canadell, J. R. Ehleringer, H. A. Mooney, O. E. Sala and E. D. Schulze (1996).  
536 "A global analysis of root distributions for terrestrial biomes." *Oecologia* **108**(3): 389-411.

537 Jian Wang, N. L., and F. Bojie. 2019. Inter-comparison of stable isotope mixing models for  
538 determining plant water source partitioning. *Science of the Total Environment*:685-693.

539 Kembel, S. W., and J. F. Cahill. 2005. Plant phenotypic plasticity belowground: A phylogenetic  
540 perspective on root foraging trade-offs. *Am Nat*:216-230.

541 Kono<sup>^</sup>пка, Bohdan, et al. "Comparison of fine root dynamics in Scots pine and Pedunculate oak  
542 in sandy soil." *Plant and Soil* 276.1-2 (2005): 33-45.

543 Law, B. E., M. G. Ryan, and P. M. Anthoni. 1999. Seasonal and annual respiration of a ponderosa  
544 pine ecosystem. *Global Change Biology* **5**:169-182.

545 Leffler, A. J., M. S. Peek, R. J. Ryel, C. Y. Ivans, and M. M. Caldwell. 2005. Hydraulic redistribution  
546 through the root systems of senesced plants. *Ecology* **86**:633-642.

547 Muler, A. L., E. J. B. van Etten, W. D. Stock, K. Howard, and R. H. Froend. 2018. Can hydraulically  
548 redistributed water assist surrounding seedlings during summer drought? *Oecologia*.

549 Nadezhdina, N., T. S. David, J. S. David, M. I. Ferreira, M. Dohnal, M. Tesař, K. Gartner, E. Leitgeb,  
550 V. Nadezhdin, J. Cermak, M. S. Jimenez, and D. Morales. 2010. Trees never rest: the  
551 multiple facets of hydraulic redistribution. *Ecohydrology* **3**:431-444.

552 Nadezhdina, N., K. Steppe, D. J. W. De Pauw, R. Bequet, J. Cermak, and R. Ceulemans. 2009. Stem-  
553 mediated hydraulic redistribution in large roots on opposing sides of a Douglas-fir tree  
554 following localized irrigation. *New Phytologist* **184**:932-943.

555 Neumann, R. B., and Z. G. Cardon. 2012. The magnitude of hydraulic redistribution by plant roots:  
556 a review and synthesis of empirical and modeling studies. *New Phytol* **194**:337-352.

557 Nippert, J. B., and R. M. Holdo. 2015. Challenging the maximum rooting depth paradigm in  
558 grasslands and savannas. *Functional Ecology* **29**:739-745.

559 Nippert, J. B., and A. K. Knapp. 2007. Soil water partitioning contributes to species coexistence in  
560 tallgrass prairie. *Oikos* **116**:1017-1029.

561 Oliveira, R. S., T. E. Dawson, S. S. Burgess, and D. C. Nepstad. 2005a. Hydraulic redistribution in  
562 three Amazonian trees. *Oecologia* **145**:354-363.

563 Oliveira, R. S., T. E. Dawson, S. S. O. Burgess, and D. C. Nepstad. 2005b. Hydraulic redistribution  
564 in three Amazonian trees. *Oecologia* **145**:354-363.

565 Parnell, A. C., D. L. Phillips, S. Bearhop, B. X. Semmens, E. J. Ward, J. W. Moore, A. L. Jackson, J.  
566 Grey, D. J. Kelly, and R. Inger. 2013. Bayesian stable isotope mixing models.  
567 *Environmetrics* **24**:387-399.

568 Priyadarshini, K., H. H. Prins, S. de Bie, I. M. Heitkönig, S. Woodborne, G. Gort, K. Kirkman, F.  
569 Ludwig, T. E. Dawson, and H. de Kroon. 2016. Seasonality of hydraulic redistribution by  
570 trees to grasses and changes in their water-source use that change tree–grass  
571 interactions. *Ecohydrology* **9**:218-228.

572 Ren, R., G. Liu, M. Wen, R. Horton, B. Li, and B. Si. 2017. The effects of probe misalignment on  
573 sap flux density measurements and in situ probe spacing correction methods. *Agricultural  
574 and Forest Meteorology* **232**:176-185.

575 Reyes-García, C., J. L. Andrade, J. L. Simá, R. Us-Santamaría, and P. C. Jackson. 2012. Sapwood to  
576 heartwood ratio affects whole-tree water use in dry forest legume and non-legume trees.  
577 *Trees* **26**:1317-1330.

578 Scholz, F. G., S. J. Bucci, G. Goldstein, M. Z. Moreira, F. C. Meinzer, J. C. Domec, R. Villalobos-Vega,  
579 A. C. Franco, and F. Miralles-Wilhelm. 2008. Biophysical and life-history determinants of  
580 hydraulic lift in Neotropical savanna trees. *Functional Ecology* **22**:773-786.

581 Scott, R. L., W. L. Cable, and K. R. Hultine. 2008a. The ecohydrologic significance of hydraulic  
582 redistribution in a semiarid savanna. *Water Resources Research* **44**.

583 Scott, R. L., W. L. Cable, and K. R. Hultine. 2008b. The ecohydrologic significance of hydraulic  
584 redistribution in a semiarid savanna. *Water Resources Research* **44**:n/a-n/a.

585 Steppe, K., D. J. W. De Pauw, T. M. Doody, and R. O. Teskey. 2010. A comparison of sap flux  
586 density using thermal dissipation, heat pulse velocity and heat field deformation  
587 methods. *Agricultural and Forest Meteorology* **150**:1046-1056.

588 Wang, G. L., C. Alo, R. Mei, and S. S. Sun. 2011. Droughts, hydraulic redistribution, and their  
589 impact on vegetation composition in the Amazon forest. *Plant Ecology* **212**:663-673.

590 Werner, R. A., and W. A. Brand. 2001. Referencing strategies and techniques in stable isotope  
591 ratio analysis. *Rapid Communications in Mass Spectrometry* **15**:501-519.

592 Williams, L. J., and E. L. Kuniandy. 2016. Revised hydrogeologic framework of the Floridan aquifer  
593 system in Florida and parts of Georgia, Alabama, and South Carolina. United States  
594 Department of the Interior, United States Geological Survey.

